

## R-L-MS-L Filter Function for CT Image Reconstruction

Huiling Hou\*, Mingquan Wang, Xiaopeng Wang

<sup>1</sup>National Key Laboratory for Electronic Measurement Technology,  
Key Laboratory of Instrumentation Science and Dynamic Measurement of Ministry of Education,  
North University of China, Taiyuan 030051, Shanxi, China

\*Corresponding author, email: hou\_huiling@126.com

### Abstract

*In X-ray computer tomography (CT), convolution back projection is a fundamental algorithm for CT image reconstruction. As filtering plays an important part in convolution back projection, the choice of filter has a direct impact upon the quality of reconstructed images. Aim at improving reconstructed image quality, a new mixed filter based on the idea of "first weighted average then linear mixing" is designed in this article, denoted by R-L-MS-L. Here, R-L filter is relied on to guarantee the spatial resolution of reconstructed image and S-L filter is processed via 3-point weighted averaging to improve the density resolution, thus enhancing the overall reconstruction quality. Gaussian noise of different coefficients is added to the projection data to contrast the noise performance of the new and traditional mixed filters. The simulation and experiment results show that the new filter is better in anti-noise performance and produces reconstructed images with notably improved quality.*

**Keywords:** CT image reconstruction; convolution back projection; filter function

**Copyright © 2016 Universitas Ahmad Dahlan. All rights reserved.**

### 1. Introduction

Today, the most popular CT technique is X-ray CT. Analytical reconstruction and iterative reconstruction are two basic techniques of CT image reconstruction. Convolution back projection is the key algorithm for analytical reconstruction. It has widely applied in commercial CT, as its good computational efficiency, good reconstructed image quality, and well parallel processing achievable by means of hardware [1, 2].

According to CT reconstruction principle, back projection is in nature painting the projection taken from a finite object space evenly back (projecting back) to each point gone through by X-ray in an infinite space, including points whose original pixel value is zero. Therefore, images reconstructed by back projection show obvious asteroid traces. A filter is needed at the output terminal in order to eliminate the asteroid traces and produce high-quality reconstructed images [3].

Common filters include R-L filter and S-L filter, using rectangular window and sinc window respectively. R-L filter is simple in form, easy to use, provides clear reconstructed image contours, and produces a high spatial resolution; however, it is affected by serious Gibbs effect [4]. S-L filter has a low oscillation response and displays some suppression effect on noises but its reconstruction quality is not as good as R-L filter when dealing with low-frequency band [5].

In an attempt to improve image reconstruction quality, scholars proposed some new filters and some mixed filters such as R-L and S-L mixed filter (denoted by R-L-S-L), R-L and NEW mixed filter, (denoted by R-L-NEW)[], etc. Mixed filters give consideration to both spatial resolution and density resolution of reconstructed images and have a good suppression effect upon noises [6, 7].

On the basis of the others, a new mixed filter denoted by R-L-MS-L is proposed using the idea of weighted average followed by linear mixing. After simulation analysis and experimentation, the new filter is proved to be strongly restraining oscillation in image reconstruction. Besides, its ant-noise performance is found improved. Thanks to the new filter, a good balance is struck between spatial resolution and density resolution for the image with a better reconstructed quality.

## 2. Design Principle of Filter

Assuming the projection data after filtering is as follows:

$$\tilde{p}(x_r, \theta) = p(x_r, \theta) * h(x_r) \quad (1)$$

Where,  $p(x_r, \theta)$  is the collected projection data,  $h(x_r)$  is the filtering function.

The ideal filter function is obtained by inverse Fourier transform, and its expression is [8]:

$$h(x_r) = \int_{-\infty}^{\infty} |\rho| \exp(i2\pi\rho x_r) d\rho \quad (2)$$

Where,  $\rho$  is the spatial frequency. Theoretically speaking, the frequency response of the filter shall be such that  $H(\rho) = |\rho|$ . The ideal filter is infinite-frequency and divergent on the infinite integral interval.

$$\int_{-\infty}^{\infty} |H(\rho)|^2 d\rho = \int_{-\infty}^{\infty} |\rho|^2 d\rho \rightarrow \infty \quad (3)$$

In accordance with Paley-Wiener theorem, such an ideal filter is unachievable. However, in practical imaging operation, if the sensor has a sampling interval small enough, the high-frequency component of sampled project data would be minimal, if not close to zero. So, the ideal filter may be processed by windowing, as follow:

$$H(\rho) = |\rho|W(\rho) \quad (4)$$

Where,  $W(\rho)$  being a window function. Realization of filtering is essentially choosing the window function  $W(\rho)$  [9].

In order to get the better reconstruction image resolution, the choice of window function should abide by certain principles:

- 1) The width of the main lobe should be narrow, so as to obtain a steep transition zone;
- 2) Relative to the main lobe, the maximum side lobe should be as small as possible, in order to improve the usual smooth degree and increase the stopband attenuation.

But generally speaking, the window function which has high and narrow main lobe, its side lobe is also projecting. Therefore, in the actual, we can not blindly requires high resolution, otherwise it will cause serious Gibbs phenomenon. In addition, the choice of window function depends on the internal structure of workpiece and actual internal components and reconstruction requirements. The most typical filtering functions are R-L filter and S-L filter.

## 3. Traditional Mixed Filters

Reference [6] proposed the R-L-S-L filter that combines the feature of R-L and S-L filters, two commonly used filters. It improves spatial resolution while minimizing image oscillation. The impulse response (sample sequence) is:

$$h_{R-L-S-L}(nd) = k_1 h_{R-L}(nd) + k_2 h_{S-L}(nd) = \begin{cases} \frac{k_1 \pi^2 + 8k_2}{4\pi^2 d^2} & , \quad n = 0 \\ \frac{-2k_2}{\pi^2 d^2 (4n^2 - 1)} & , \quad n \text{ is even} \\ -\frac{k_1}{n^2 \pi^2 d^2} - \frac{2k_2}{\pi^2 d^2 (4n^2 - 1)} & , \quad n \text{ is odd} \end{cases} \quad (5)$$

Where,  $h_{R-L}(nd)$  and  $h_{S-L}(nd)$  are the spatial domain expression of R-L and S-L filters respectively,  $k_1$  and  $k_2$  are weighted coefficients, with  $k_1 + k_2 = 1$ .

Reference [7] proposed R-L-NEW filter by mixing R-L and NEW filter. It is expressed as below:

$$h_{R-L-NEW}(nd) = k_1 h_{R-L}(nd) + k_2 h_{NEW}(nd)$$

$$= \begin{cases} \frac{k_1}{4d^2} + \frac{k_2}{6d^2} & , \quad n = 0 \\ \frac{-k_2}{2\pi^2 d^2 n^2} & , \quad n \text{ is even} \\ \frac{-k_1}{\pi^2 d^2 n^2} - \frac{k_2}{2\pi^2 d^2 n^2} & , \quad n \text{ is odd} \end{cases} \quad (6)$$

Where,  $h_{R-L}(nd)$  and  $h_{NEW}(nd)$  are the spatial domain expression of R-L and NEW filters respectively,  $k_1$  and  $k_2$  are weighted coefficients, with  $k_1 + k_2 = 1$ .

With respect to image reconstruction, we usually use two indices, spatial resolution and density resolution, to evaluate the reconstructed image quality. Here, spatial resolution is the ability to identify the smallest object on CT images. Density resolution refers to discriminating detected objects by means of image gray scale. Generally speaking, when the main lobe is higher and narrower, a better spatial resolution can be gain. The smaller the side lobe and the quicker the convergence, the higher the density resolution of the image would be. At a given set of projection data, the two indices are conflicting. Table 1 gives the width and amplitude ( $d=1\text{mm}$ ) of the main lobe and the first side lobe expressed by spatial domain curves of the above filtering functions after Fourier transformation. Both mixed filters take  $k_1 = 0.5$  and  $k_2 = 0.5$ .

Table 1. Amplitude and width of the main lobe and the first side lobe

Filter	Main lobe height	Main lobe width	First side lobe height	First side lobe width
R-L	0.25	1.42	-0.101	0.389
S-L	0.202	1.498	-0.067	0.232
R-L-S-L	0.226	1.532	-0.084	0.227
R-L-NEW	0.187	1.456	-0.051	0.201

It is found from Table 1 that when the mixed filters give a better and balanced consideration to spatial resolution and density resolution of reconstructed images compared with traditional R-L and S-L filters. The R-L-NEW mixed filter is the best in table1. When comparing filters in the remainder of this article, we will compare a new mixed filter with the R-L-New mixed filter.

### 3.1. A New Mixed Filter

When designing a new filter, we would attempt to give better consideration to both spatial and density resolutions so as to improve the overall reconstruction quality.

Firstly, start out with S-L filter function to design a new filter function using the idea of weighted average. Its basic rationale is performing weighted average of the points in the neighborhood starting from null field filtering function and using signal and system viewpoints, so as to shorten the main lobe and diminish the side lobe and improve the density resolution at the expense of the spatial resolution. There is a certain restriction relationship between spatial resolution and density resolution. in view of the specific situation, choose the right priorities. In view of the specific situation, choose the right priorities. The appropriate emphasis will be determined In view of the specific circumstances [10, 11].

Classical S-L filter has the following sampling sequence:

$$h_{s-L}(nd) = \frac{-2}{\pi^2 d^2 (4n^2 - 1)}, n = 0, \pm 1, \pm 2, \dots \tag{7}$$

Theoretically, a translation in the spatial domain, when represented in frequency domain, is multiplication by an fluctuation factor  $e^{i2\pi pk/(2N-1)}$ ; and when there are  $2n-1$  points in the spatial neighborhood for weighted averaging, it is expressed in frequency domain as below:

$$H(\rho) = \sum_{k=-n}^n (-1)^k w_k |\rho| W_{s-L}(\rho) \exp\left(\frac{i2\pi k}{2N-1}\right) \tag{8}$$

Where,  $N$  is the sampling frequency in the null field;  $\sum_{k=-n}^n W_k = 1$  is the normalized expression.  $W_k$  may be modified to suit specific situation.

By the research, averaging has a smoothing effect on reconstructed images, but more than 3-point weighted averaging would distort and blur the edge of reconstructed images. We process S-L filter via 3-point weighted averaging, denoted by MS-L filter, whose sampling sequence is:

$$h_{MS-L}(nd) = 0.2h_{s-L}(nd - d) + 0.6h_{s-L}(nd) + 0.2h_{s-L}(nd + d) \tag{9}$$

The corresponding time domain is represented as:

$$h_{MS-L}(nd) = \frac{-0.4}{\pi^2 d^2 (4(n-1)^2 - 1)} + \frac{-1.2}{\pi^2 d^2 (4n^2 - 1)} + \frac{-0.4}{\pi^2 d^2 (4(n+1)^2 - 1)}, n = 0, \pm 1, \pm 2, \dots \tag{10}$$

Figure 1 and 2 are the discrete distribution of the main lobe and the far side lobe of R-L and MS-L filtering functions respectively.

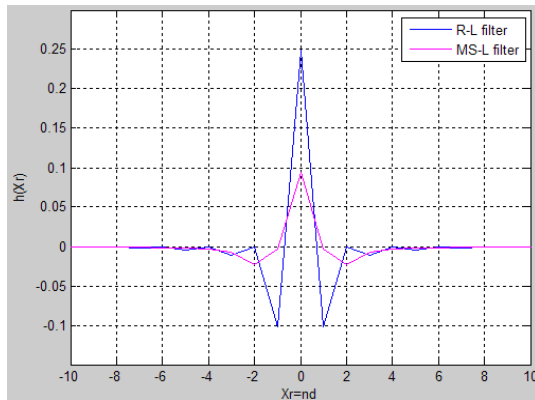


Figure 1. Main lobe of R-L and MS-L in spatial domain

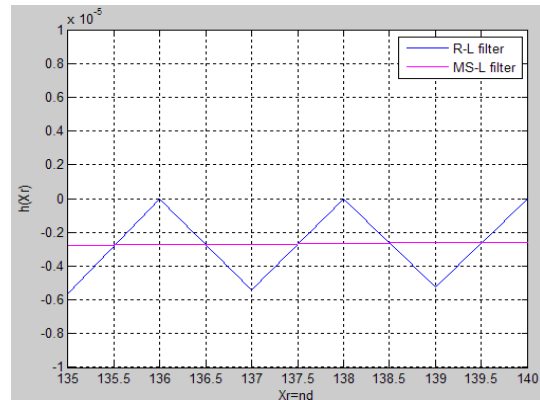


Figure 2. Far side lobe of R-L and MS-L in spatial domain

Figure 1 shows that the main lobe of R-L filter is higher and narrower, indicating good spatial resolution, but its side lobe is larger in amplitude and width, signifying severe Gibbs effect; while MS-L filter function produces a short and wide main lobe. Figure 2 shows that convergence effect of its far side lobe is not very well, indicating poor spatial resolution; while MS-L filter has higher rate of convergence, which helps suppress Gibbs effect and noises. It can be obtained by Figure 1 and Figure 2 that when designing a mixed filter, we may rely on R-L filter to guarantee the spatial resolution of reconstructed image and use MS-L filter to improve

the density resolution. The new mixed filter is denoted by R-L-MS-L. Its response function is as follow:

$$h_{R-L-MS-L}(t) = k_1 h_{R-L}(t) + k_2 h_{MS-L}(t) \quad (11)$$

Where,  $k_1 \geq 0, k_2 \geq 0, k_1 + k_2 = 1$ . The value of  $k_1$  and  $k_2$  is adjustable. When  $k_1 = 0$ , it becomes an R-L filter; when  $k_2 = 0$  it becomes an MS-L filter. Its sampling sequence is:

$$h_{R-L-MS-L}(nd) = \begin{cases} \frac{k_1}{4d^2} + \frac{14k_2}{15\pi^2 d^2} & , \quad n=0 \\ h_{MS-L}(nd) & , \quad n \text{ is even} \\ -\frac{k_1}{n^2 \pi^2 d^2} - k_2 h_{MS-L}(nd) & , \quad n \text{ is odd} \end{cases} \quad (12)$$

#### 4. Experimental Simulation and Result Analysis

Parallel beam reconstruction is performed on 2D Shepp-Logan model [5] using respectively R-L filter, R-L-New mixed filter, and the filter designed in this article. In order to evaluate reconstructed image quality in the presence of noises, Gaussian noise with 5% intensity are added into the projection data, the mean and variance being 0 and 1 respectively.

Figure 3 shows the original Shepp-Logan model and its gray curve of line 128. Figure 4-6 show reconstructed results of R-L, R-L-New, and R-L-MS-L filter and their respective gray curve of line 128.

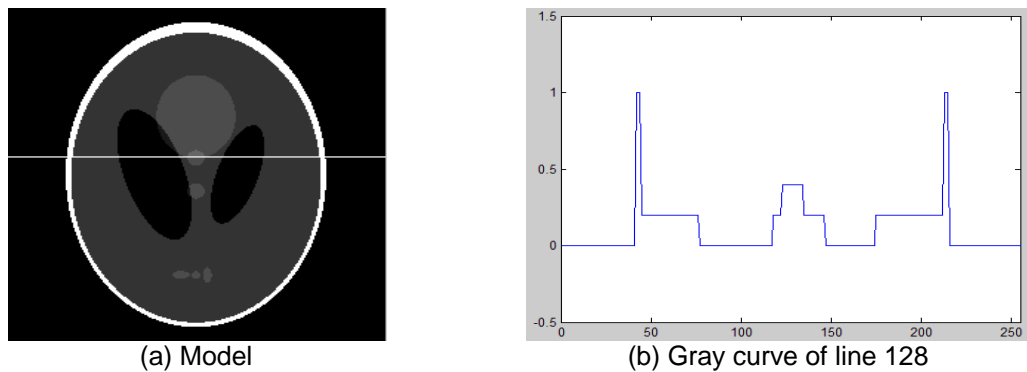


Figure 3. Original model

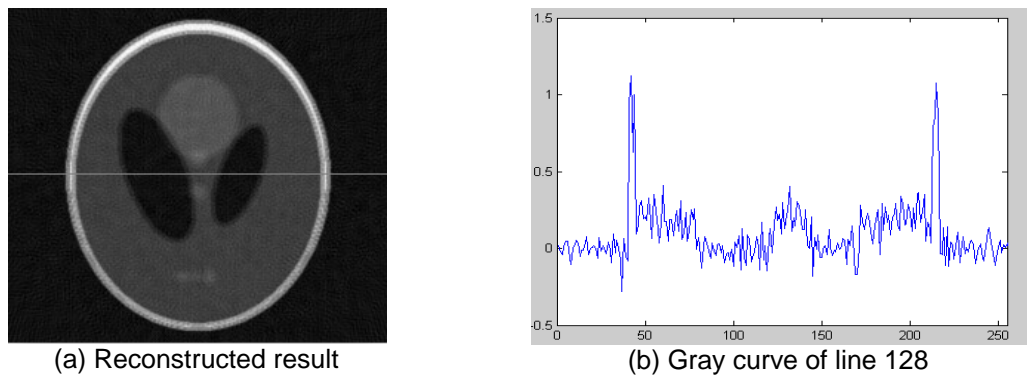


Figure 4. Reconstructed result of R-L filter

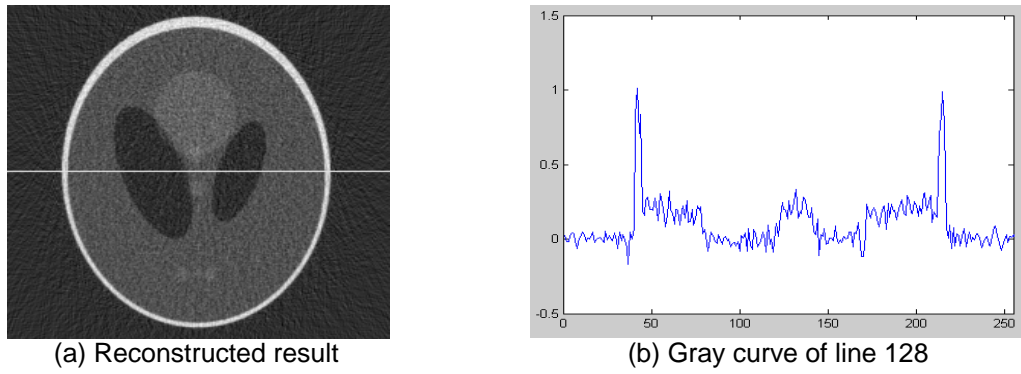


Figure 5. Reconstructed result of R-L-New filter

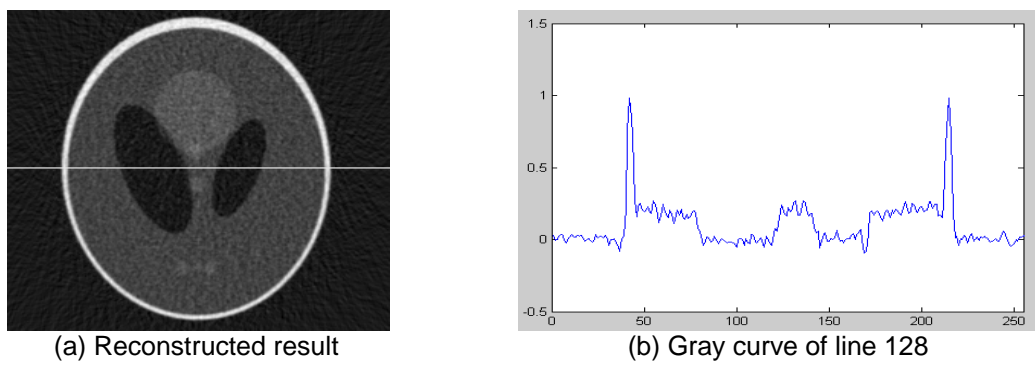


Figure 6. Reconstructed result of R-L-MS-L filter

By comparing Figure 3 to Figure 6, we find that the new filter performs better than R-L filter and R-L-New filter in that its reconstructed image is not only smoother but also closer to the original image.

For the sake of evaluating reconstructed image quality of different filters in a more objectively manner, we use two evaluation functions, namely normalized mean square distance  $d$  and normalized mean absolute distance  $r$  [12]. They are expressed by:

$$d = \left[ \frac{\sum_{u=1}^N \sum_{v=1}^N (t_{u,v} - r_{u,v})^2}{\sum_{u=1}^N \sum_{v=1}^N (t_{u,v} - \bar{t})^2} \right]^{\frac{1}{2}} \tag{13}$$

$$r = \frac{\sum_{u=1}^N \sum_{v=1}^N |t_{u,v} - r_{u,v}|}{\sum_{u=1}^N \sum_{v=1}^N t_{u,v}} \tag{14}$$

Where,  $t_{u,v}$  and  $r_{u,v}$  are respectively the test model and the pixel density of various reconstructed points.  $\bar{t}$  is the average value of test model density.  $d$  is sensitive to the great error of a few points, as a great error of individual points may lead to a great  $d$  value. Whereas  $r$  reveals sensitively the small errors of more points. Images reconstructed by different filters are assessed using the above two distance indices. The assessment results are given in Table 2.

The results indicate that the new filter performs generally better and reconstructs higher quality image under the same noise condition.

Table 2. Normalized distances of three filters under the same noise intensity

Filter	5% intensity		10% intensity	
	$d$	$r$	$d$	$r$
R-L filter	0.4818	0.5992	0.8331	1.1182
R-L-New Filter	0.4191	0.4949	0.6496	0.8279
R-L-MS-L Filter	0.3738	0.4094	0.5125	0.6258

What needs illustrating is the choice of  $k_1$  and  $k_2$  in Equation 11. As  $k_1 + k_2 = 1$ , we study the influence of  $k_1$  to R-L-MS-L filter function by selecting different  $k_1$  values to reconstruct. The relationship between  $k_1$  and normalized mean square distance is shown in Figure 7. It can be seen that the best value of  $k_1$  is 0.7 or so to be better inhibiting oscillation and noise.

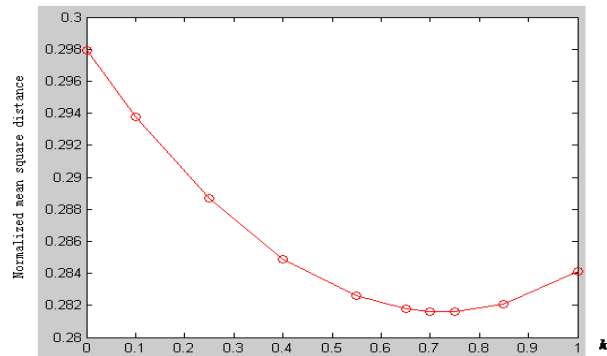


Figure 7. The relationship between  $k_1$  and normalized mean square distance

FDK reconstruction is performed on 360 pictures of 1024\*1024 rocket motor model projection data acquired by the lab. Figure 8 shows the sinogram of the reconstruction data. Figure 9(a) and 9(b) are the 150th slice image reconstructed by R-L-New filter and the new filter. It is readily seen that the image reconstructed by R-L-MS-L filter has clearer details and better image quality.

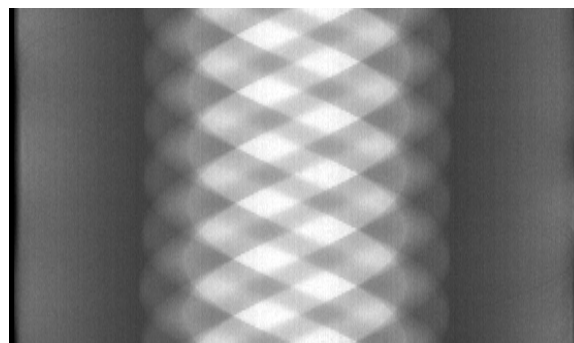


Figure 8. The sinogram of reconstruction data

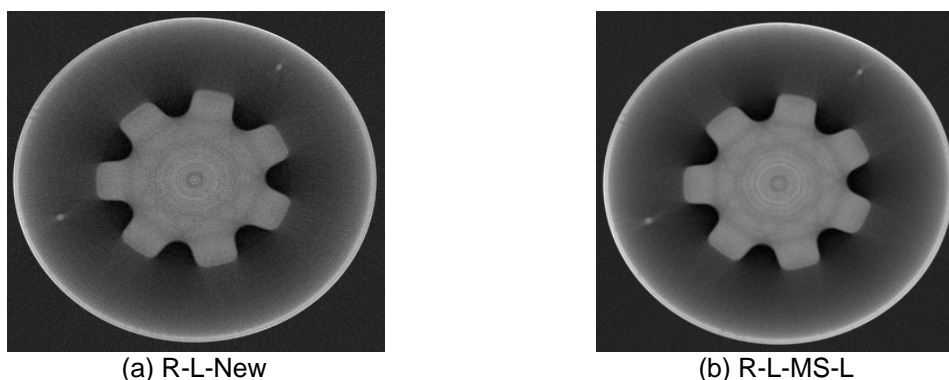


Figure 9. Comparison of FDK using different filters

## 5. Conclusion

In this article, we design a new filter named R-L-MS-L filter, based on the idea of weighted averaging and linear mixing. Experimentation and simulation show that R-L-MS-L filter does better in image reconstruction than traditional filters, because it not only strongly restrains the oscillation in image reconstruction but also has better noise immunity. The new filter improves the image density resolution significantly while ensuring the spatial resolution of the reconstructed image. Good reconstruction results are achieved both in 2D CT reconstruction and 3D CT reconstruction.

## Acknowledgements

This work is supported by the National Natural Science Foundation of china (No.61171177).

## References

- [1] Shi Hongli, Luo Shuqian. A novel scheme to design the filter for CT reconstruction using FBP algorithm. *BioMedical Engineering Online*, 2013; 12(1): 50-65.
- [2] Yang Meng, Yan Peimin, Huang Hui, Li Jifei. *Filtered back projection reconstruction research based on Gaussian in PET images*. 2012 International Conference on Audio, Language and Image Processing, Proceedings. Shanghai. 2012; 1: 360-364.
- [3] Bilgot Anne, Desbat Laurent, Perrier Valérie. *FBP and the interior problem in 2D tomography*. 2011 IEEE Nuclear Science Symposium and Medical Imaging Conference(NSS/MIC). Valencia. 2012; 1: 4080-4085.
- [4] Ramachandrana GN, Lakshminarayanan AV, Kolaskara AS. Theory of the non-planar peptide unit. *Biochimica et Biophysica Acta (BBA) - Protein Structure*, 1973, 303(2): 385-388.
- [5] Sheep L A, Logan B F. The Fourier reconstruction of a head section. *IEEE trans. Nucl. Sci.* 1974; 21(1): 21-43
- [6] Zhai Jing, Pan Jinxiao, Liu Bin. Application of Mixed Filter Function in FDK Algorithm. *Journal of Nanchang Hangkong University (Nature Science)*. 2007, 21(1): 263-266
- [7] Zhang Bin. Pan Jinxiao. A new type of mixed filters for CT image reconstruction. *Microcomputer Information*. 2009; 25(3): 298-308
- [8] Wei Yu Chuan, Wang Ge, Hsieh Jian. An Intuitive Discussion on the Ideal Ramp Filter in Computed Tomography. *Computers and Mathematics with Applications*. 2005; 49(5-6): 731-740.
- [9] Ren Zhong, Liu Guodong, Huang Zhen. *Improvement of wavelet threshold filtered back-projection image reconstruction algorithm*. Proceedings of SPIE-The International Society for Optical Engineering. Beijing. 2014; 9301: 1-10
- [10] Xie Hui, Duan Wanchun, Sun Yonghe, Du Yuanwei. Dynamic DEMATEL group decision approach based on intuitionistic fuzzy number. *Telkomnika (Telecommunication Computing Electronics and Control)*. 2014; 12(4): 1064-1072
- [11] Shi Benyi, Wang Cheng, Chen Sihai, Bi Kun. A Novel Method of CT Reconstruction Filter Function Design. *CT Theory and Applications*. 2010; 19(4): 35-43
- [12] Ji Dongjiang, He Wenzhang. *The correction SART algorithm based on circular symmetrical object*. 2009 International Conference on Computational Intelligence and Security. Beijing. 2009; 1: 151-154.